



The orientation dependence of transformation strain of Ni–Mn–Ga polycrystalline alloy and its composite with epoxy resin

B. Tian^a, F. Chen^a, Y.X. Tong^a, L. Li^a, Y.F. Zheng^{a,b,*}, Y. Liu^{a,c}

^a Center for Biomedical Materials and Engineering, Harbin Engineering University, Harbin 150001, China

^b Department of Advanced Materials and Nanotechnology, College of Engineering, Peking University, Beijing 100871, China

^c School of Mechanical Engineering, The University of Western Australia, Crawley WA6009, Australia

ARTICLE INFO

Article history:

Received 5 May 2010

Received in revised form 5 June 2010

Accepted 12 June 2010

Available online 25 June 2010

Keywords:

Metals and alloys
Composite materials
Phase transitions
Shape memory
Anisotropy

ABSTRACT

This study investigated the transformation strains of Ni–Mn–Ga polycrystalline alloy and Ni–Mn–Ga/epoxy resin composites. For the Ni–Mn–Ga polycrystalline alloy, the columnar grains formed along the solidification direction, and the alloy expanded during martensitic transformation in the direction with a transformation strain of ~500 ppm. For the composite consisting of randomly distributed Ni–Mn–Ga particles, no transformation strain was achieved due to the random distribution of the Ni–Mn–Ga particles. For the composite consisting of properly oriented Ni–Mn–Ga particles, the martensitic transformation strains were found to be orientation-dependent, the shrinking transformation strain-*c* (parallel to the direction of magnetic field used during curing) up to ~210 ppm was detected, and the expanding transformation strain-*a* (vertical to the direction of magnetic field used during curing) was measured to be ~150 ppm.

© 2010 Elsevier B.V. All rights reserved.

1. Introduction

Ni–Mn–Ga ferromagnetic shape memory alloy (FSMA) has been widely investigated due to its ability to exhibit large magnetic-field-induced strains (MFIS) [1]. A MFIS of up to 6–10% [2,3] has been reported in a single crystal Ni–Mn–Ga alloy. However, as a Heusler metallic compound, Ni–Mn–Ga polycrystalline alloy has great inherent brittleness that significantly hinders its practical applications. To overcome this problem, the polymer composites with Ni–Mn–Ga particles have been developed [4–7], in which the polymer matrix provides the integrity and ductility whereas the Ni–Mn–Ga particles produce the desired function. It has been reported that Ni–Mn–Ga particle/polymer composites exhibit good shape recovery [4] and large mechanical energy absorption [5]. The composite with properly oriented Ni–Mn–Ga particles shows larger energy absorption efficiencies than the composite with randomly distributed particles [5]. This indicates that some properties of Ni–Mn–Ga particle/polymer composite are closely dependent on the orientation of the particles. In this work, the original Ni–Mn–Ga bulk polycrystalline alloy and the epoxy resin matrix composites with randomly distributed and properly oriented Ni–Mn–Ga FSMA

particles are prepared and their thermal induced strain properties are investigated.

2. Experimental details

A polycrystalline $\text{Ni}_{49.8}\text{Mn}_{28.5}\text{Ga}_{21.7}$ alloy ingot was prepared by arc melting in argon atmosphere from high purity elements. The solidified ingot was homogenized at 1123 K for 10 h in vacuum followed by water-quenching. The grains of the alloy might grow during the homogenization process and the phase transformation strain property of the alloy should be enhanced due to the homogenization of composition in the process. The homogenized ingot was crushed into grits with size ~3 mm and then milled for 4 h in a QM-1SP4 planetary ball mill. The ball milling process had been described in detail earlier [8,9], in which it was found that the effect of mechanical alloying on the alloy was not generated during the ball milling process because of the short milling time. The as-milled powders with particle size ranging from 5 μm to 50 μm were sealed in quartz tube under high vacuum and annealed at 1023 K for 2 h to restore the ferromagnetism and martensitic transformation [9].

The composite was fabricated by mixing the annealed $\text{Ni}_{49.8}\text{Mn}_{28.5}\text{Ga}_{21.7}$ alloy powders and bisphenol-A epoxy resin (E-44, brand in China). Triethylene-tetramine was used as the hardener for curing the epoxy resin. Firstly, the epoxy resin was heated to 333 K in a beaker using a water bath to decrease its viscosity. Then 50 wt.% of Ni–Mn–Ga powder was added into the resin and the mixture was manually stirred with glass rod for 10 min followed by ultrasonication for 10 min. Subsequently, the hardener was added into the mixture and mechanically stirred gently to avoid the entrapment of air bubbles. Afterwards, the mixture was poured into a mold of 60 mm \times 7 mm \times 4 mm in dimension followed by ultrasonication for 15 min to eliminate residual air bubbles. The cast was allowed to cure at room temperature for 24 h, either in the ambient to create isotropic composite or in a magnetic field of ~1800 Oe along the width direction of the mold to create aligned composite [10]. Finally the cast was subjected to a post-curing treatment for 2 h at 373 K.

The martensitic transformation and magnetic transition of the Ni–Mn–Ga bulk alloy, powder and particle/epoxy resin composites were determined by measuring the temperature dependence of low-field ac magnetic susceptibility. The fracture

* Corresponding author at: Department of Advanced Materials and Nanotechnology, College of Engineering, Peking University, Beijing 100871, China.
Tel.: +86 10 6276 7411; fax: +86 10 6276 7411.

E-mail address: yfzheng@pku.edu.cn (Y.F. Zheng).

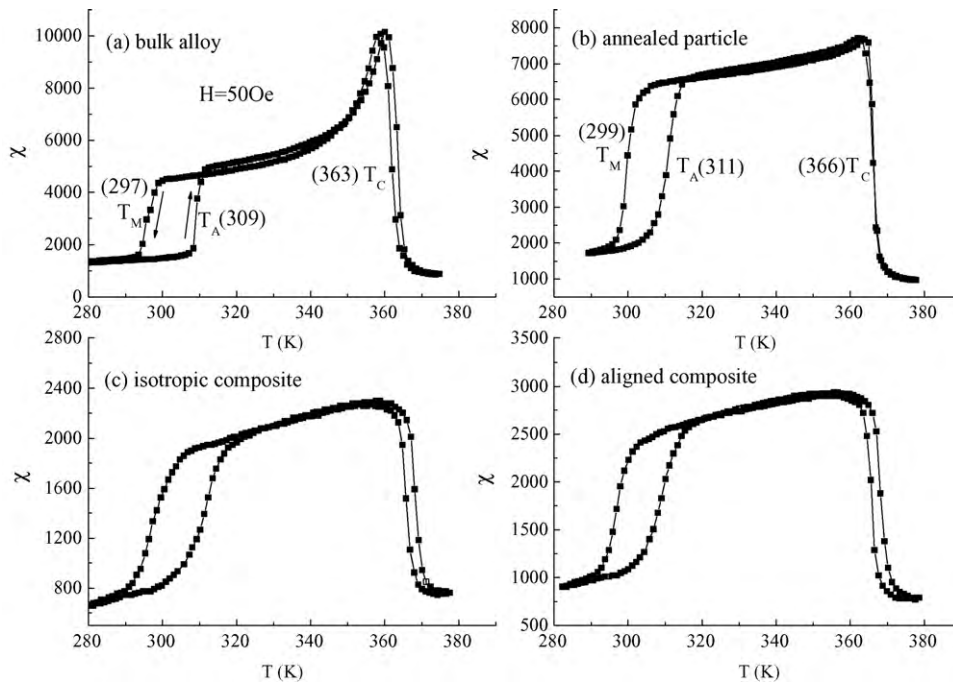


Fig. 1. Low-field χ - T curves for (a) $\text{Ni}_{49.8}\text{Mn}_{28.5}\text{Ga}_{21.7}$ bulk alloy, (b) annealed $\text{Ni}_{49.8}\text{Mn}_{28.5}\text{Ga}_{21.7}$ alloy particles, (c) isotropic $\text{Ni}_{49.8}\text{Mn}_{28.5}\text{Ga}_{21.7}$ alloy particle/epoxy resin composite and (d) aligned $\text{Ni}_{49.8}\text{Mn}_{28.5}\text{Ga}_{21.7}$ alloy particle/epoxy resin composite.

surface of the Ni-Mn-Ga bulk alloy was observed using a Cambridge-S240 scanning electron microscope (SEM). X-ray diffraction (XRD) was carried out at room temperature to identify the orientation of grains in the bulk alloy using a Panalytical X-pert PRO diffractometer with $\text{Cu K}\alpha$ radiation. Magnetic hysteresis loops were measured using a physics property measurement system (PPMS) manufactured by Quantum Corporation. Thermal induced transformation strain for Ni-Mn-Ga bulk alloy and Ni-Mn-Ga/epoxy resin composites were recorded using a multi-parameter magnetic measurement system manufactured by the Institute of Physics, Chinese Academy of Sciences, in which the strain gauge was adhered to the sample to measure the strain. Samples with dimension of $3\text{ mm} \times 3\text{ mm} \times 3\text{ mm}$ were cut for the measurement of transformation strains.

3. Results and discussion

Fig. 1 shows the ac susceptibility as a function of temperature for the different samples in a field of 50 Oe. For the $\text{Ni}_{49.8}\text{Mn}_{28.5}\text{Ga}_{21.7}$ bulk alloy, it can be seen that an abrupt increase of susceptibility at $\sim 363\text{ K}$ upon cooling corresponds to the Curie transition of the austenite, as shown in Fig. 1(a). Continuous cooling to $\sim 297\text{ K}$ causes a sudden decrease of susceptibility, indicating the starting of austenite \rightarrow martensite transformation. Upon heating, the increase of susceptibility at $\sim 309\text{ K}$ represents the occurrence of martensite \rightarrow austenite transformation. The temperatures at the maximum slope (middle point) of the curves are defined as the austenite \rightarrow martensite, martensite \rightarrow austenite and Curie transition temperatures, marked as T_M , T_A and T_C , respectively. The sharp decrease of susceptibility upon cooling from 360 K to 340 K is due to the effect of stress anisotropy caused by high level of quenched-in stresses and strong magneto-elastic coupling in Ni-Mn-Ga bulk alloys [11]. The T_M , T_A and T_C temperatures of the annealed Ni-Mn-Ga particles are slightly higher ($\sim 2\text{ K}$) than those of the Ni-Mn-Ga bulk alloy, as shown in Fig. 1(b). It is seen that, upon cooling from 360 K to 340 K , the susceptibility shows less change with temperature. This may mean that annealing at 1023 K for 2 h favors reducing the effect of stress anisotropy in the $\text{Ni}_{49.8}\text{Mn}_{28.5}\text{Ga}_{21.7}$ powder, consistent with the previous report [9]. Fig. 1(c) and (d) are for the isotropic composite and composite with aligned $\text{Ni}_{49.8}\text{Mn}_{28.5}\text{Ga}_{21.7}$ particles, respectively. It is clear that the T_M , T_A and T_C temperatures of the two composites are close to

those of the annealed Ni-Mn-Ga alloy powder. Moreover, the susceptibilities of these two composites are much lower than that of the annealed Ni-Mn-Ga alloy particles because of the existence of non-magnetic epoxy resin matrix.

Fig. 2(a) shows the SEM image of the fracture surface for the $\text{Ni}_{49.8}\text{Mn}_{28.5}\text{Ga}_{21.7}$ bulk alloy. The surface is just parallel to the solidification direction in the arc melting preparation process. The

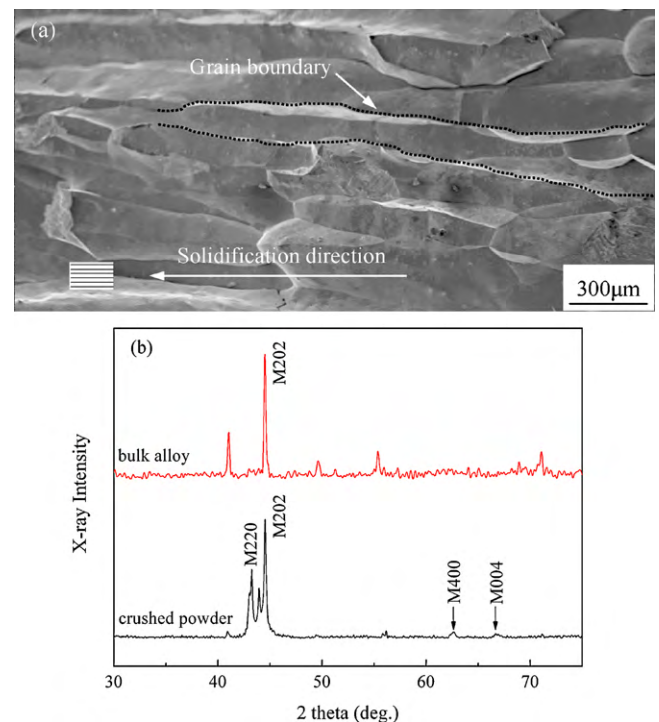


Fig. 2. (a) SEM micrograph of fractured surface along solidification direction for the $\text{Ni}_{49.8}\text{Mn}_{28.5}\text{Ga}_{21.7}$ bulk alloy and (b) XRD patterns of the bulk alloy and the crushed $\text{Ni}_{49.8}\text{Mn}_{28.5}\text{Ga}_{21.7}$ alloy powder samples.

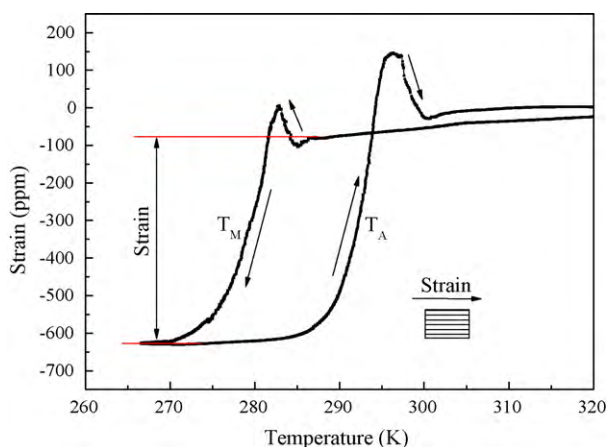


Fig. 3. Strain–temperature curve for the $\text{Ni}_{49.8}\text{Mn}_{28.5}\text{Ga}_{21.7}$ bulk alloy.

columnar grains formed along the solidification direction, which is attributed to the strong temperature gradient of this direction resulting from the contact between water-cooled copper crucible and the ingot. The width of some grains, as indicated in the figure, may reach up to $\sim 150\ \mu\text{m}$. Liu et al. [12] reported a similar structure with the grain width of $\sim 100\ \mu\text{m}$ in a polycrystalline $\text{Ni}_{45.2}\text{Mn}_{36.7}\text{In}_{13}\text{Co}_{5.1}$ alloy prepared by arc melting method, and the grains in that alloy exhibit a well-developed preferred orientation along the solidification direction. The XRD was performed on the above fracture surface to identify the orientation of grains in the present Ni–Mn–Ga alloy, with the result being shown in Fig. 2(b), in which the result of the crushed Ni–Mn–Ga alloy powder is given for comparison. As compared to the powder sample, the characteristic diffraction peaks of [2 2 0], [4 0 0] and [0 0 4] for the martensite phase in the bulk alloy disappeared, with only [2 0 2] peak remained. According to the results, it is assumed that the grains in the bulk alloy form a fiber texture in the solidification direction. These indicate that the grains may have a preferred orientation along the direction, similar to the result in the polycrystalline $\text{Ni}_{45.2}\text{Mn}_{36.7}\text{In}_{13}\text{Co}_{5.1}$ alloy [12].

The sample for the strain measurement was cut from the annealed button alloy along the solidification direction. The positive and negative strain should correspond to the shrinkage and expansion of the sample in the present study, respectively. Fig. 3 shows the strain–temperature curve for the $\text{Ni}_{49.8}\text{Mn}_{28.5}\text{Ga}_{21.7}$ bulk alloy. The strain was measured along the columnar grain direction. The sample shrinks slightly ~ 100 ppm during cooling from 285 K to 282 K and then expands abruptly ~ 600 ppm from 282 K to 270 K on cooling due to the austenite \rightarrow martensite transformation. Therefore, the net expanding transformation strain of the martensitic transformation is ~ 500 ppm. Upon heating, the sample nearly recovers its original shape via shrinking from 284 K to 296 K and expanding from 296 K to 300 K, which indicates the martensite \rightarrow austenite transformation. It is seen that the strain is recovered by reverse transformation via two different deformation types.

In general, the martensitic transformation often occurs with self-accommodation of twin variants to minimize the free energy of the alloy. If a complete self-accommodation behavior takes place, the alloy will not generate a strain during the transformation. Therefore, for the polycrystalline alloy, it should fulfill two conditions for generating a transformation strain. Firstly, the martensitic variants within the grains in the alloy are not self-accommodated completely during martensitic transformation. Secondly, the grains in the alloy should have a consistent orientation, which provides a large macro-strain by the accumulation of the strains generated by each grain. It is believed that the residual internal stress caused

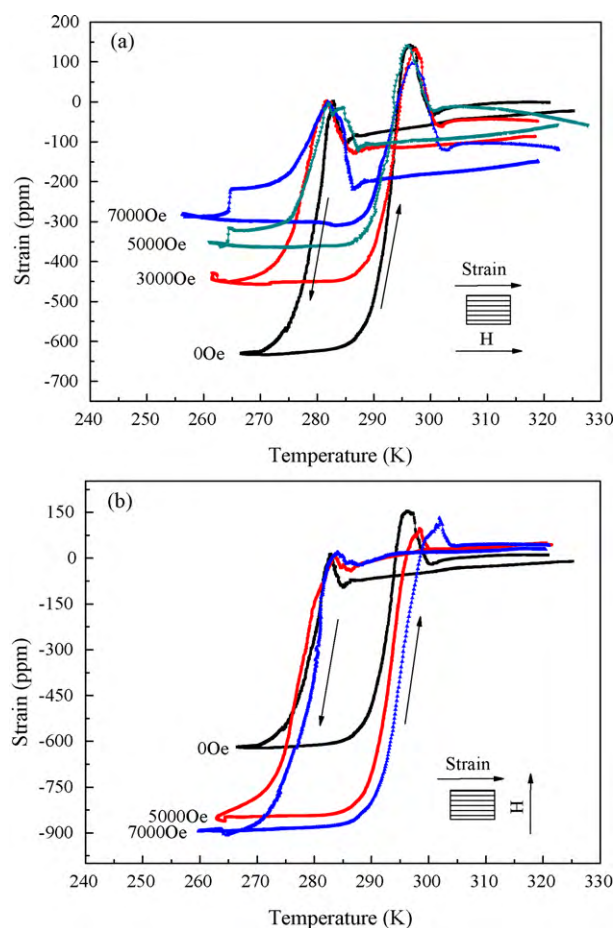


Fig. 4. Strain–temperature curves for the bulk alloy measured with different bias magnetic filed: (a) parallel and (b) vertical to the columnar grain direction.

by the directional solidification during growth would make the martensitic variants get preferential orientation [13]. Therefore, for the present $\text{Ni}_{49.8}\text{Mn}_{28.5}\text{Ga}_{21.7}$ polycrystalline alloy, the intrinsic degree of self-accommodation of martensitic variants is reduced, which supports the first condition. As described in Fig. 2, the columnar grains in the $\text{Ni}_{49.8}\text{Mn}_{28.5}\text{Ga}_{21.7}$ bulk alloy may have similar orientation along the direction of solidification, which makes the second condition satisfied. Thus, a ~ 500 ppm transformation strain is obtained in the present $\text{Ni}_{49.8}\text{Mn}_{28.5}\text{Ga}_{21.7}$ polycrystalline alloy.

Fig. 4(a) shows the influence of external magnetic field on the transformation strain of the bulk alloy. The magnetic field is parallel to the strain direction during martensitic transformation and removed when the transformation completes. In addition, no magnetic field is performed during the reverse transformation. It is seen that, with the increase of magnetic field, the expanding strain of martensitic transformation is reduced gradually. When the bias magnetic field is rotated to the lateral direction, the expanding strain of martensitic transformation increased with increasing the magnetic field, as shown in Fig. 4(b). These results indicate that the magnetic field subjected during the martensitic transformation makes the alloy contract in the magnetic field direction. As we know, the external magnetic field will make the sample contract in the magnetic field direction due to the growth of variants with the easy magnetization axis c (short axis) in the direction at the expense of the other variants via martensitic twin boundary motion (mechanism of MFIS). Therefore, the MFIS of the alloy with martensite phase should be responsible for the effect of external magnetic field on the martensitic transformation strain.

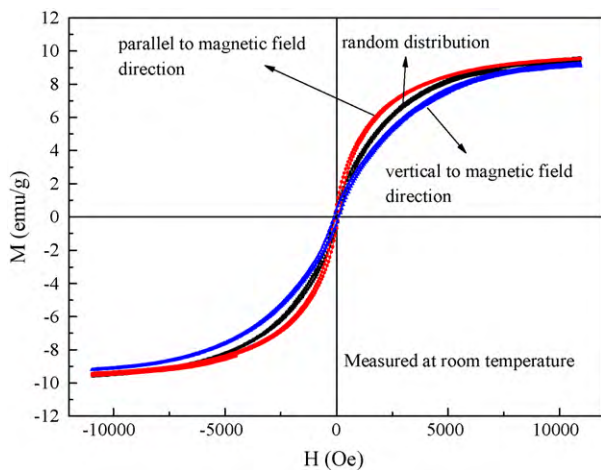


Fig. 5. The magnetization loops for the $\text{Ni}_{49.8}\text{Mn}_{28.5}\text{Ga}_{21.7}$ alloy particle/epoxy resin composite cured without magnetic field (random distribution (black line)) and $\text{Ni}_{49.8}\text{Mn}_{28.5}\text{Ga}_{21.7}$ alloy particle/epoxy resin composite cured with magnetic field (parallel to magnetic field direction (red line) and vertical to magnetic field direction (blue line)). (For interpretation of the references to color in this figure legend, the reader is referred to the web version of the article.)

Based on the above discussion, it is concluded that the preferred orientation of grains in the bulk alloy is a critical precondition for achieving a transformation strain. This is also applicable for the composite. In this study, the composites are cured with or without external magnetic field to create anisotropic or isotropic arrangement of Ni–Mn–Ga particles [10]. For analyzing the orientation of particles in the two composites, the magnetization test as an effective method [6] is performed. As can be seen from Fig. 5, the magnetizations of these two composites are nearly saturated to the same value up to 10,000 Oe. However, at the low magnetic field range (0–5000 Oe), as compared to the composite without magnetic field during curing, the composite cured with magnetic field shows an easy magnetization behavior in the magnetic field direction and a hard magnetization behavior in the lateral direction. This confirms that the external magnetic field is effective to control the orientation of the Ni–Mn–Ga particles, which is consistent with the XRD result in our previous report [10].

Fig. 6 shows the strain–temperature curves of the composite with oriented Ni–Mn–Ga particles. The transformation strain along and perpendicular to the magnetic field direction are denoted strain-c and strain-a, respectively. Fig. 6(a) shows the strain-c variation with temperature for the composite. It is seen that the composite contracts at 295–280 K for the austenite \rightarrow martensite transformation and expands at 290–302 K for the martensite \rightarrow austenite transformation. The full transformation strain is ~ 210 ppm. Strain-a shows an opposite dependence on temperature, as shown in Fig. 6(b). These facts indicate that the strain response for the composite is orientation-dependent. The absolute value of strain-a is ~ 150 ppm, smaller than that of strain-c. The transformation strains of the composite are comparatively smaller than that of the Ni–Mn–Ga bulk alloy. Different from the composite with oriented particles, the composite with randomly distributed Ni–Mn–Ga alloy particles does not show any phase transformation strain upon cooling and heating.

For the Ni–Mn–Ga particle/epoxy resin composite, every Ni–Mn–Ga particle embedded in the epoxy resin matrix can exhibit a deformation with phase transformation like the above described Ni–Mn–Ga bulk alloy due to the existence of residual internal stress introduced by ball milling. For the composite containing randomly distributed Ni–Mn–Ga alloy particles, the deformation direction of Ni–Mn–Ga alloy particle is random and the strains caused by all particles are statistically cancelled, resulting in a nil total shape

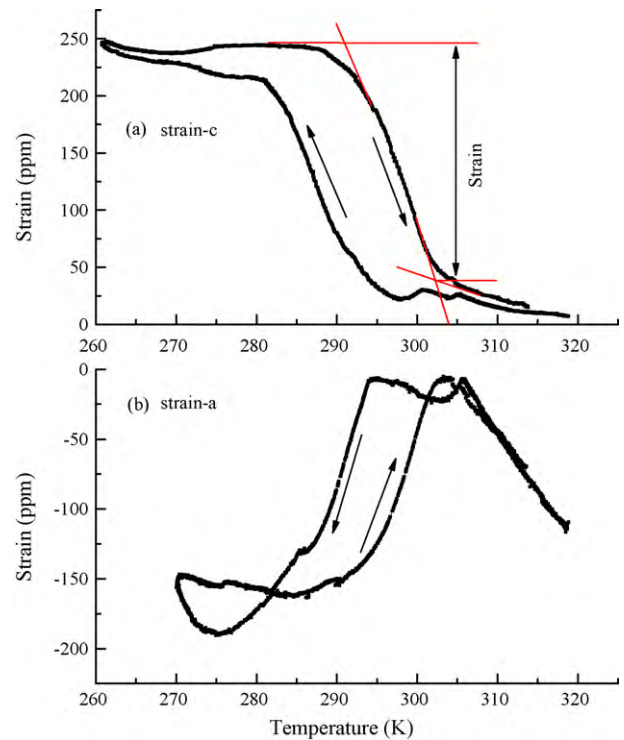


Fig. 6. Strain–temperature curves for the oriented $\text{Ni}_{49.8}\text{Mn}_{28.5}\text{Ga}_{21.7}$ alloy particle/epoxy resin composite: (a) strain-c (strain parallel to the magnetic field direction) and (b) strain-a (strain perpendicular to the magnetic field direction).

change. For the composite with oriented Ni–Mn–Ga alloy particles, each Ni–Mn–Ga alloy particle exhibits the same deformation direction and the accumulation of deformation caused by all particles results in the strain of the whole composite. The relatively smaller transformation strain of composite than that of the bulk alloy should result from the low content of Ni–Mn–Ga alloy in the composite.

4. Conclusions

- (1) The Ni–Mn–Ga bulk alloy, particles and composites containing randomly distributed particles and oriented particles exhibit close characteristic temperatures for martensitic transformation, austenitic transformation and Curie transformation.
- (2) The Ni–Mn–Ga bulk polycrystalline alloy shows an expanding strain of ~ 500 ppm in the columnar grain direction during martensitic transformation. It is found that the expanding strain decreases with the increase of magnetic field parallel to the strain direction, which should be attributed to the MFIS of the alloy in the martensite state.
- (3) The composite consisting of randomly distributed Ni–Mn–Ga alloy particles does not show transformation strain. For the composite consisting of oriented particles, it exhibits a different transformation strain depending on the orientation direction. The composite shrinks ~ 210 ppm in the strain-c direction and expands ~ 150 ppm in the strain-a direction during martensitic transformation.

References

- [1] K. Ullakko, J.K. Huang, C. Kantner, R.C. O'Handley, V.V. Kokorin, *Appl. Phys. Lett.* 69 (1996) 1966–1968.
- [2] S.J. Murray, M. Marioni, S.M. Allen, R.C. O'Handley, *Appl. Phys. Lett.* 77 (2000) 886–888.
- [3] A. Sozinov, A.A. Likhachev, N. Lanska, K. Ullakko, *Appl. Phys. Lett.* 80 (2002) 1746–1748.

- [4] H. Hosoda, S. Takeuchi, T. Inamura, K. Wakashima, *Sci. Technol. Adv. Mater.* 5 (2004) 503–509.
- [5] J. Feuchtwanger, M.L. Richard, Y.J. Tang, A.E. Berkowitz, R.C. O'Handley, S.M. Allen, *J. Appl. Phys.* 97 (10) (2005) M319.
- [6] N. Scheerbaum, D. Hinz, O. Gutfleisch, K.-H. Müller, L. Schultz, *Acta Mater.* 55 (2007) 2707–2713.
- [7] M. Lahelin, I. Aaltio, O. Heczko, O. Söderberg, Y. Ge, B. Löfgren, S.-P. Hannula, J. Seppälä, *Compos. Part A* 40 (2009) 125–129.
- [8] B. Tian, F. Chen, Y. Liu, Y.F. Zheng, *Mater. Lett.* 62 (2008) 2851–2854.
- [9] B. Tian, F. Chen, Y. Liu, Y.F. Zheng, *Intermetallics* 16 (2008) 1279–1284.
- [10] B. Tian, F. Chen, Y.X. Tong, L. Li, Y.F. Zheng, *Mater. Lett.* 63 (2009) 1729–1732.
- [11] R. Tickle, R.D. James, J. Magn. Magn. Mater. 195 (1999) 627–638.
- [12] J. Liu, S. Aksoy, N. Scheerbaum, M. Acet, O. Gutfleisch, *Appl. Phys. Lett.* 95 (2009) 232515.
- [13] W.H. Wang, G.H. Wu, J.L. Chen, C.H. Yu, Z. Wang, Y.F. Zheng, L.C. Zhao, W.S. Zhan, *J. Phys.: Condens. Matter* 12 (2000) 6287–6293.